CrystEngComm

COMMUNICATION

View Article Online
View Journal | View Issue

Cite this: *CrystEngComm*, 2015, **17**, 8207

Received 18th August 2015,
Accepted 18th September 2015

DOI: 10.1039/c5ce01662b

www.rsc.org/crystengcomm

Structural, morphological and optical investigation of β-Ag_2MoO_4 microcrystals obtained with different polar solvents†

F. S. Cunha,[a] J. C. Sczancoski,[b] I. C. Nogueira,[c] V. G. de Oliveira,[a] S. M. C. Lustosa,[a] E. Longo[b] and L. S. Cavalcante*[a]

This communication reports the formation of beta-silver molybdate (β-Ag_2MoO_4) microcrystals synthesized by a simple precipitation method using different polar solvents (water, methanol, ethanol, 1-propanol and 1-butanol). These crystals were structurally characterized by means of X-ray diffraction (XRD) and Rietveld refinement. The crystal shapes and sizes were observed by field emission scanning electron microscopy (FE-SEM). Their optical properties were analyzed by ultraviolet-visible (UV-vis) diffuse reflectance spectroscopy. XRD patterns and Rietveld refinement data indicated all crystals have a spinel-type cubic structure. FE-SEM images revealed the crystals tend to increase the average size with reduction in the degree of polarity of the solvent. Finally, β-Ag_2MoO_4 microcrystals exhibited a dependence of optical band gap energies (from 3.22 to 3.38 eV) on the intermediary energy levels.

Silver molybdate (Ag_2MoO_4) presents two types of electronic structure, depending on the pressure conditions in which the crystal is subjected.[1] At room temperature, Ag_2MoO_4 exhibits a spinel-type cubic structure related to beta phase (β-Ag_2MoO_4), which is more stable in nature. However, when exposed to high hydrostatic pressure, these crystals have a tetragonal structure associated to alpha metastable phase (α-Ag_2MoO_4).[2] Recently, the literature[3] has reported the formation of α-Ag_2MoO_4 metastable phase by a solution-phase precipitation method under ambient conditions using 3-bis(2-pyridyl)pyrazine (dpp) as dopant.[3] The influence of pH value of the starting solution on the growth and formation processes of distinct heterostructures (brooms, flowers and rods) was investigated by Singh *et al.*[4] and Fodjo *et al.*,[5] in which sodium borohydride was employed to induce the reduction of silver nanoparticles on the surface of Ag_2MoO_4 crystals in order to enhance Raman scattering. In other study, Ag–Ag_2MoO_4 composites prepared by microwave-assisted hydrothermal synthesis presented interesting photocatalytic activity for the degradation of Rhodamine B under visible light.[6] In addition, Ag_2MoO_4 mixed with graphite acts as a good lubricant for Ni-based composites, improving the tribological properties of this system.[7]

Different synthesis methods have been employed to obtain pure β-Ag_2MoO_4 crystals, including solid-state reaction using an oxide mixture at high temperature,[8] melt-quenching[9] and Czochralski growth.[10] Particularly, high temperatures, long processing times, and/or sophisticated equipment are necessary in these synthetic routes. Moreover, the final products may be composed of particles having irregular shapes with non-homogeneous size distribution as well as contain secondary phases. In recent years, pure β-Ag_2MoO_4 crystals have been synthesized by co-precipitation,[11] microwave-assisted hydrothermal synthesis,[11,12] dynamic template route through polymerization of acrylamide-assisted templates[13] and the impregnation/calcination method.[14] Due to the peculiarity of each synthetic route with the experimental conditions, β-Ag_2MoO_4 crystals are able to exhibit different physicochemical properties, as photoluminescence, photocatalysis, antibacterial action against the DH5α bacteria and catalytic oxidation of elemental mercury, respectively.

However, little attention has been given in the literature to the formation of β-Ag_2MoO_4 crystals using different chemical solvents in the reaction medium. Therefore, in this communication, β-Ag_2MoO_4 microcrystals were synthesized by the precipitation method, employing several polar solvents, as deionized water (H_2O), methanol (CH_4O), ethanol (C_2H_6O), 1-propanol (C_3H_8O) and 1-butanol ($C_4H_{10}O$) at 60 °C for 8 h. X-ray diffraction (XRD), Rietveld refinement and field emission scanning electron microscopy (FE-SEM) were employed for structural and morphological characterization. The optical properties were investigated by ultraviolet-visible diffuse reflectance spectroscopy with evaluation of the optical band gap values.

[a] *PPQG-DQ-CCN-Universidade Estadual do Piauí, Rua João Cabral, CP 2231, 64002-150, Teresina, PI, Brazil. E-mail: laeciosc@bol.com.br*
[b] *Universidade Estadual Paulista, CP 355, 14801-907, Araraquara, SP, Brazil*
[c] *PPG em Engenharia de Materiais, Instituto Federal do Maranhão, 65030-005, São Luís, MA, Brazil*

† Electronic supplementary information (ESI) available. See DOI: 10.1039/c5ce01662b

The experimental procedure and characterization of β-Ag_2MoO_4 microcrystals are described in ESI.†

Fig. 1(a–e) illustrate the XRD patterns of the β-Ag_2MoO_4 microcrystals prepared at 60 °C for 8 h with different polar solvents.

XRD patterns in Fig. 1(a–e) confirmed all β-Ag_2MoO_4 crystals have a spinel-type cubic structure, without any deleterious phase, with the space group $Fd\bar{3}m$ and point-group symmetry O_h^7, in good agreement with ICSD card no. 36187 (ref. 15) and the literature.[16] The sharp and intense diffraction peaks are typical features of a structurally ordered material at long-range. On the other hand, the low detection limit imposed by the XRD technique does not allow the existence of less than 2% or the absence of any trace of Ag phase to be estimated, if it exists in the form of Ag nanoparticles grown on the surface of β-Ag_2MoO_4 microcrystals.[16–18] The dipole moment (μ) of each polar solvent used in the syntheses is displayed in Table S1.† Particularly, the decrease in μ values promoted the narrowing of the diffraction peak widths and the change in Ag–O and Mo–O bond angles (Table S1 in ESI†).

The Rietveld method is based on the construction of diffraction patterns calculated according to a structural model.[19] The calculated patterns are adjusted to fit the observed patterns and thus, provide the structural parameters of the material and diffraction profile. In our study, Rietveld refinement was used to adjust the atomic positions, lattice parameters, and unit cell volume. All refinements were performed using the general structure analysis (GSAS) program.[20] Again, the structural refinements confirmed all β-Ag_2MoO_4 microcrystals have a spinel-type cubic structure without secondary phases (Fig. S1 and Table S2 in the ESI†).

Fig. 2 shows a schematic representation of a β-Ag_2MoO_4 structure modeled by means of Rietveld refinement data.

The lattice parameters and atomic positions estimated from Rietveld refinements were employed to model this structure by the Visualization for Electronic and Structural Analysis (VESTA) program (version 3.3.1 for Windows).[21] The spinel-type cubic structure of β-Ag_2MoO_4 microcrystals is characterized by the space group $Fd\bar{3}$m with eight molecular formulae per unit cell (Z = 8).[15] In these structures, silver atoms are coordinated to six oxygens forming octahedral [AgO_6] clusters. The molybdenum atoms are coordinated to four oxygens, which result in tetrahedral [MoO_4] clusters. In principle, our Rietveld refinement data, especially the anisotropic displacement parameters (U) in Table S2 (ESI†), indicate the existence of distorted octahedral [AgO_6] clusters and undistorted tetrahedral [MoO_4] clusters.

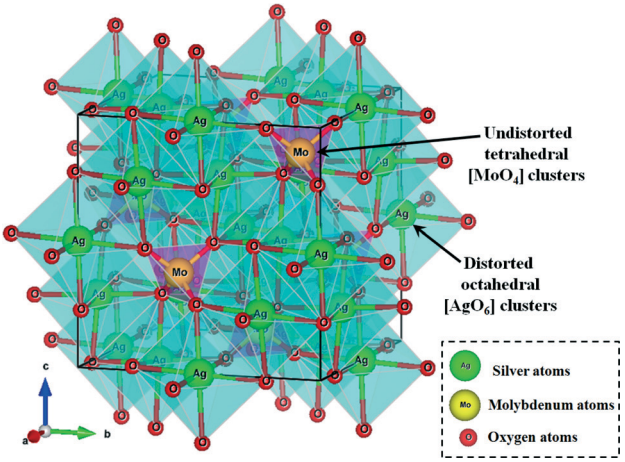

Fig. 2 Schematic representation of cubic β-Ag_2MoO_4 structure.

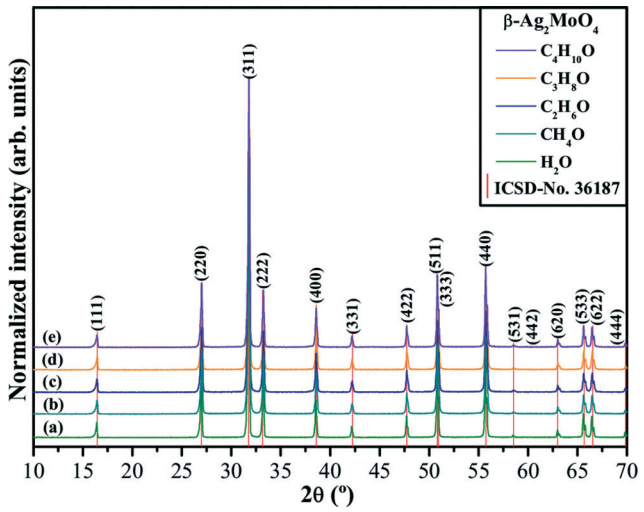

Fig. 1 XRD patterns of β-Ag_2MoO_4 microcrystals prepared with (a) H_2O, (b) CH_4O, (c) C_2H_6O, (d) C_3H_8O and (e) $C_4H_{10}O$.

Fig. 3(a–c) show the electron density models in the (001), (010) and (1$\bar{1}$0) planes of β-Ag_2MoO_4 crystals, respectively.

These electron density models were calculated by the Fourier transform of structure factors from the structural parameters and atomic scattering factors of free atoms obtained from Rietveld refinement for the β-Ag_2MoO_4 crystals at 60 °C for 8 h using H_2O as solvent. These data were used in the VESTA program[21] to model the electron density map. In these figures, a color scale on each plane is displayed, which demonstrates zones with high and low electronic densities. In Fig. 3(a), the blue colored regions are related to the absence of an electronic charge, while the red colored areas exhibit a high electronic density. Moreover, it is possible to verify if the four Ag–O chemical bonds located on the a- and b-axes ($d_{x^2-y^2}$ orbitals) exhibit a slight atomic displacement, which suggests the existence of distortions (Fig. 3(a)). In the (010) plane, only two Mo atoms are found, in which the green area around the Mo atoms indicates the presence of four O atoms with short bond distances (Fig. 3(b)). Finally, it is revealed that in the (1$\bar{1}$0) plane, Ag and Mo atoms are able to share the same oxygen, in which the bond distance between O–Ag–O is higher than that between O–Mo–O.

Fig. 4(a–e) show the FE-SEM images and Fig. 4(f) illustrates average crystal size of β-Ag_2MoO_4 microcrystals prepared with different polar solvents.

The micrographs in Fig. 4(a–e) suggest a dependence of the crystal shape on the type of solvent. In principle, the

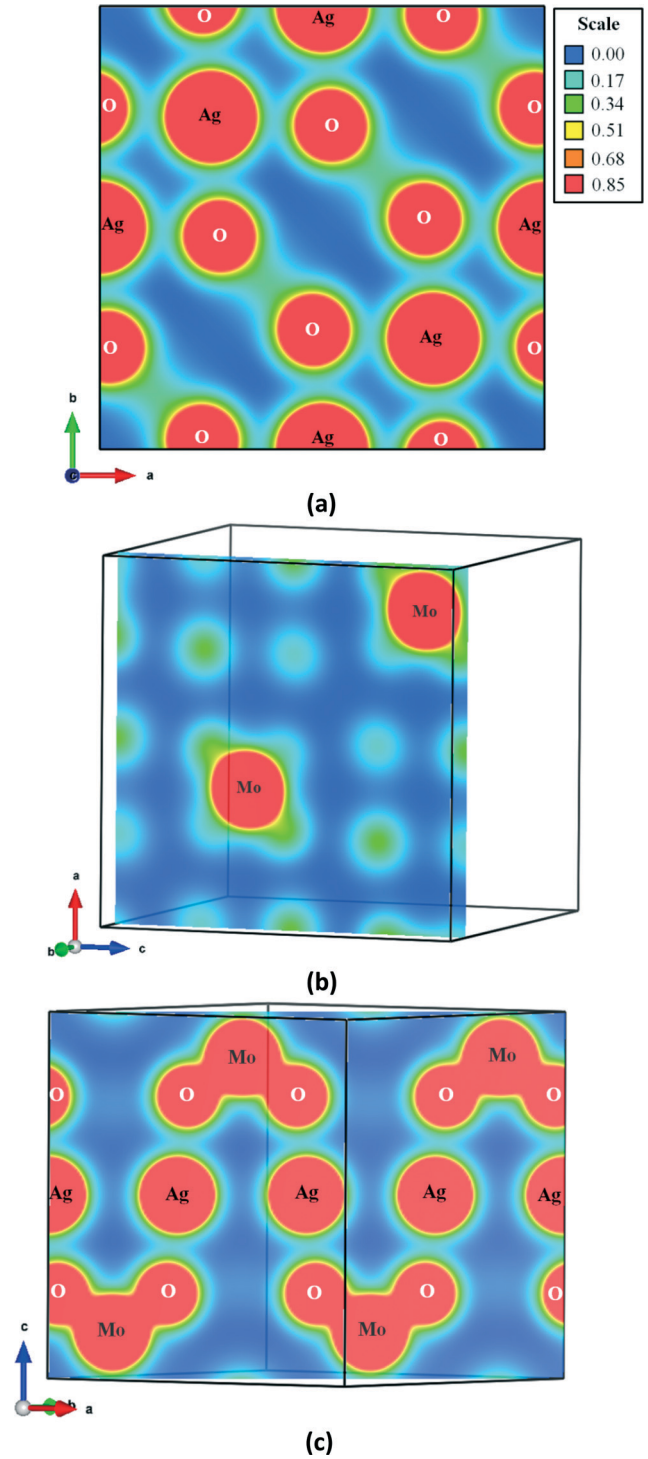

Fig. 3 Electron density maps on the (a) (001), (b) (010) and (c) (1$\bar{1}$0) planes of β-Ag_2MoO_4 microcrystals.

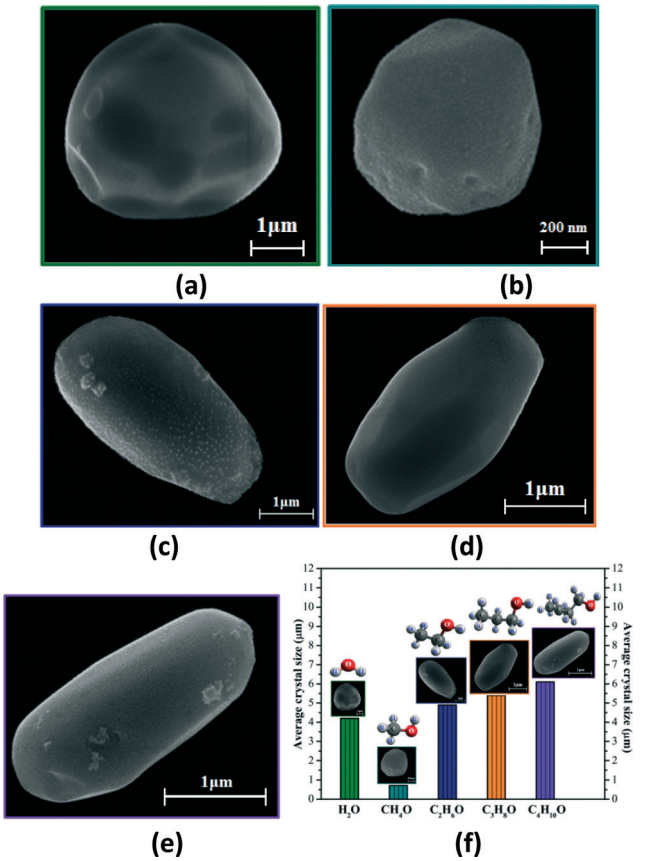

Fig. 4 FE-SEM micrographs of individual β-Ag_2MoO_4 microcrystals prepared with (a) H_2O, (b) CH_4O, (c) C_2H_6O, (d) C_3H_8O and (e) $C_4H_{10}O$, and (f) dependence of average crystal size as a function of the type of solvent.

increase in alcohol chain changes the crystal shape from irregular quasi-spherical (H_2O and CH_4O) to elongated crystals (C_2H_6O, C_3H_8O and $C_4H_{10}O$). The smallest crystal size was noted for the samples prepared with the CH_4O solvent (Fig. 4(b)), which can be related to its high saturated vapor pressure. This solvent with a low boiling point (64.7 °C), when employed as a reaction medium, promotes a weak interaction between the nuclei and favors the formation of small quasi-spherical β-Ag_2MoO_4 crystals.[22] Some Ag nanoparticles grew on the surface of β-Ag_2MoO_4 microcrystals due to the accelerated electron beam from the field emission scanning electron microscope under high vacuum, a phenomenon that has already been elucidated and discussed in previous papers.[16] Another important information observed in these micrographs was the increase in average crystal size of β-Ag_2MoO_4 microcrystals with the decrease of solvent polarity (Fig. 4(f)). This result is in good agreement with the FE-SEM images of β-Ag_2MoO_4 microcrystals illustrated in Fig. S2 (ESI†). Therefore, the type of solvent is able to affect the morphological behavior of the system, especially the formation and growth stages of primary nanoparticles. In addition, preferential growth occurs for the crystals formed using the C_2H_6O, C_3H_8O and $C_4H_{10}O$ solvents, as a type of template effect.

The optical band gap energy (E_{gap}) of β-Ag_2MoO_4 crystals was estimated by a modified Kubelka–Munk equation:[23–25]

$$[F(R_\infty)h\nu] = C_1(h\nu - E_{gap})^n \quad (1)$$

where $F(R_\infty)$ is the Kubelka–Munk function, R_∞ is the reflectance ($R_\infty = R_{sample}/R_{standard}$; $R_{standard}$ was magnesium oxide [MgO]), $h\nu$ is the photon energy, C_1 is a proportionality

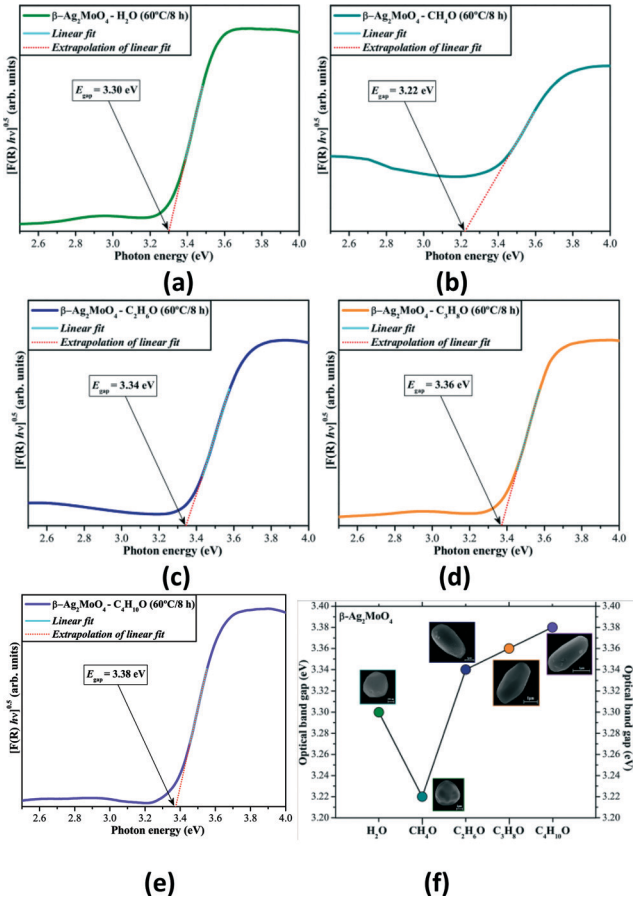

Fig. 5 UV-vis diffuse reflectance spectra of β-Ag_2MoO_4 microcrystals prepared with different polar solvents: (a) H_2O, (b) CH_4O, (c) C_2H_6O, (d) C_3H_8O and (e) $C_4H_{10}O$. (f) Evolution of the optical band gap (E_{gap}) values of all microcrystals.

constant, E_{gap} is the optical band gap and n is a constant associated with different types of electronic transitions (n = 0.5 for a direct allowed, n = 2 for an indirect allowed, n = 1.5 for a direct forbidden and n = 3 for an indirect forbidden). For the β-Ag_2MoO_4 microcrystals, the optical absorption spectra are governed by indirect electronic transitions.[12] In these typical physical phenomena, after the electronic absorption process, the electrons located in the minimum energy states in the conduction band (CB) are able to go back to the maximum energy states in the valence band (VB), but in distinct points in the Brillouin zone.[26] Based on this information, the E_{gap} values of β-Ag_2MoO_4 microcrystals were calculated by applying n = 2 in eqn (1).

Therefore, after obtaining the $F(R_\infty)$ value from eqn (1) and plotting a graph of $[F(R_\infty)h\nu]^2$ as a function of $h\nu$, the E_{gap} values for the β-Ag_2MoO_4 microcrystals were estimated by extrapolating the linear portion of UV-vis curves.

Fig. 5(a–f) show the UV-vis diffuse reflectance spectra and optical band gap (E_{gap}) values of the β-Ag_2MoO_4 microcrystals synthesized in this study.

In Fig. 5(a–f), significant changes in the E_{gap} values of β-Ag_2MoO_4 microcrystals were not verified, except for the crystals formed with the CH_4O solvent. Although the E_{gap} estimated by UV-vis measurements is considered qualitative, the calculated results imply that the microcrystals have distinct types and concentrations of structural and surface defects, such as oxygen vacancies, distortions on the O–Ag–O bonds, and porous surfaces. All these defects arise from the crystal formation and growth processes, which are influenced by the type of solvent used in the synthesis, as well as the irreversible attachment (agglomeration) caused by the dynamics of particle–particle collisions. Consequently, these defects cause a symmetry break responsible for the lattice polarization, resulting in the presence of intermediary energy levels within the band gap.[27] Thus, the microcrystals synthesized with CH_4O (lower E_{gap}) have a lower density of intermediary energy states than the microcrystals prepared with the other solvents.

In summary, monophasic β-Ag_2MoO_4 microcrystals were synthesized with different polar solvents (H_2O, CH_4O, C_2H_6O, C_3H_8O and $C_4H_{10}O$) by a simple precipitation method at 60 °C for 8 h. XRD patterns indicated all crystals are structurally ordered at long-range. Rietveld refinement data confirmed all microcrystals have a spinel-type cubic structure, which is composed of distorted octahedral [AgO_6] clusters and undistorted tetrahedral [MoO_4] clusters. Electron density models were employed to understand the polarization phenomenon and anisotropic atomic displacements in [O–Ag–O] bonds. FE-SEM images showed a dependence of the formation and growth stages of these microcrystals on the type of polar solvent employed in the synthesis. The slight differences in E_{gap} values were caused by the existence of intermediary energy states within the band gap. These energetic states originated from the defects, which differ in type and concentration between the microcrystals. We expect that this facile and controllable synthetic route can be used in the preparation of new complex metal oxides for future technological applications in solid-state lighting, solar cells, sensors, fuel cells and photocatalysis.

Acknowledgements

The Brazilian authors acknowledge the financial support from the Brazilian research financing institutions CNPq (120482/2014-2, 350711/2012-7 and 479644/2012-8), FAPESP (12/14004-5 and 13/07296-2) and CAPES.

Notes and references

1 A. K. Arora, R. Nithya, S. Misra and T. Yagi, *J. Solid State Chem.*, 2012, **196**, 391.
2 A. Beltrán, L. Gracia, E. Longo and J. Andrés, *J. Phys. Chem. C*, 2014, **118**, 3724.
3 C. H. B. Ng and W. Y. Fan, *Cryst. Growth Des.*, 2015, **15**, 3032.
4 D. P. Singh, B. Sirota, S. Talpatra, P. Kohli, C. Rebholz and S. M. Aouadi, *J. Nanopart. Res.*, 2012, **14**, 781.

5 E. K. Fodjo, D. W. Li, N. P. Marius, T. Albert and Y. T. Long, *J. Mater. Chem. A*, 2013, **1**, 2558.
6 Z. Q. Li, X. T. Chen and Z. L. Xue, *Sci. China: Chem.*, 2013, **56**, 443.
7 E. Liu, Y. Gao, J. Jia and Y. Bai, *Tribol. Lett.*, 2013, **50**, 313.
8 S. A. Suthanthiraraj and Y. D. Premchand, *Ionics*, 2004, **10**, 254.
9 F. Rocca, A. Kuzmin, P. Mustarelli, C. Tomasi and A. Magistris, *Solid State Ionics*, 1999, **121**, 189.
10 S. Brown, A. Marshall and P. Hirst, *Mater. Sci. Eng., A*, 1993, **173**, 23.
11 Y. V. B. De Santana, J. E. C. Gomes, L. Matos, G. H. Cruvinel, A. Perrin, C. Perrin, J. Andrès, J. A. Varela and E. Longo, *Nanomater. Nanotechnol.*, 2014, **4**, 22.
12 A. F. Gouveia, J. C. Sczancoski, M. M. Ferrer, A. S. Lima, M. R. M. C. Santos, M. S. Li, R. S. Santos, E. Longo and L. S. Cavalcante, *Inorg. Chem.*, 2014, **53**, 5589.
13 H. Jiang, J. K. Liu, J. D. Wang, Y. Lu and X. H. Yang, *CrystEngComm*, 2015, **17**, 5511.
14 S. Zhao, Z. Li, Z. Qu, N. Yan, W. Huang, W. Chen and H. Xu, *Fuel*, 2015, **158**, 891.
15 R. W. G. Wyckoff, *J. Am. Chem. Soc.*, 1922, **44**, 1994.
16 J. Andrés, M. M. Ferrer, L. Gracia, A. Beltran, V. M. Longo, G. H. Cruvinel, R. L. Tranquilin and E. Longo, *Part. Part. Syst. Charact.*, 2015, **32**, 646.
17 E. Longo, L. S. Cavalcante, D. P. Volanti, A. F. Gouveia, V. M. Longo, J. A. Varela, M. O. Orlandi and J. Andrés, *Sci. Rep.*, 2013, **3**, 1676.
18 L. S. Cavalcante, M. A. P. Almeida, Jr., W. Avansi, R. L. Tranquilin, E. Longo, N. C. Batista, V. R. Mastelaro and M. S. Li, *Inorg. Chem.*, 2012, **51**, 10675.
19 H. M. Rietveld, *Acta Crystallogr.*, 1967, **22**, 151.
20 A. C. Larson and R. B. von Dreele, *General structure analysis system (GSAS)*, Los Alamos: National Laboratory, 2001, p. 124.
21 K. Momma and F. Izumi, *J. Appl. Crystallogr.*, 2011, **44**, 1272.
22 K. G. Kanade, B. B. Kale, R. C. Aiyer and B. K. Das, *Mater. Res. Bull.*, 2006, **41**, 590.
23 P. Kubelka and F. Munk, *Z. Tech. Phys.*, 1931, **12**, 593.
24 A. E. Morales, E. S. Mora and U. Pal, *Rev. Mex. Fis. S*, 2007, **53**, 18.
25 R. A. Smith, *Semiconductors*, Cambridge University Press, London, 2nd edn, 1978, p. 434.
26 R. Lacomba-Perales, J. Ruiz-Fuertes, D. Errandonea, D. Martínez-García and A. Segura, *EPL*, 2008, **83**, 37002.
27 V. S. Marques, L. S. Cavalcante, J. C. Sczancoski, A. F. P. Alcântara, M. O. Orlandi, E. Moraes, E. Longo, J. A. Varela, M. S. Li and M. R. M. C. Santos, *Cryst. Growth Des.*, 2010, **10**, 4752.